# Exploring the versatility of liquid phase exfoliation: Producing 2D nanosheets from talcum powder, cat litter and beach sand

Andrew Harvey,[1] John B. Boland,[1] Ian Godwin,[1] Adam G Kelly,[1] Beata M. Szydłowska,[1] Ghulam Murtaza,[2] Andrew Thomas,[3] David J. Lewis,[4] Paul O'Brien[2] and Jonathan N Coleman[1*]

[1]*School of Physics, CRANN and AMBER Research Centres, Trinity College Dublin, Dublin 2, Ireland*

[2]*School of Chemistry, The University of Manchester, Manchester, M13 9PL, United Kingdom*

[3]*School of Materials and Photon Science Institute, The University of Manchester, Manchester, M13 9PL, United Kingdom*

[4]*School of Materials, The University of Manchester, Manchester, M13 9PL, United Kingdom*

**colemaj@tcd.ie*


ABSTRACT: Liquid phase exfoliation (LPE) has proven to be a versatile technique to produce uncharged 2D nanosheets from layered crystals. However, almost all studied starting materials consist of pure powder or crystals purchased from chemical suppliers. To test the true versatility of this process, we have attempted to process three starting materials with varying degrees of purity and composition. We subjected talcum powder (principle component, the layered compound talc), Fuller's earth cat litter (known to contain layered silicate compounds, most notably palygorskite and montmorillonite/bentonite) and beach sand (suspected to contain small amounts of layered clays) to a standard LPE procedure (sonication in a surfactant solution followed by centrifugation). In all cases, we produced dispersions containing large quantities of nanosheets with almost all non-nanosheet material removed by the centrifugation step. Powder X-ray diffraction identified the nanosheets produced to be talc, a bentonite/palygorskite mixture and mica for the three starting materials respectively. Particularly interesting is the fact that bentonite, palygorskite and mica sheets are charged and

are always accompanied by charge balancing counterions. We believe this is the first example of LPE being used to exfoliate and purify charged layered crystals.

## Introduction

Due to their interesting properties and broad potential for applications, 2-dimensional materials have been intensively studied over the last few years.[1-3] For a number of applications in fields such as composites,[4] printed electronics[5] and electrochemical devices,[6] it will be necessary to produce suspensions of nanosheets in liquids. A number of methods exist to do this, with well-known examples being oxidation of graphite to give graphene oxide, ion intercalation-mediated exfoliation of $MoS_2$ or ion-exchange assisted exfoliation of layered double hydroxides.[2] However all of these methods are relatively narrow in that they tend to apply to a single material or family of materials. In contrast, one exfoliation route, generally termed liquid phase exfoliation, is known to be quite versatile and widely applicable.[7, 8] This method is a top-down route to produce few-layer nanosheets by shearing[9] or ultrasonication[10] of layered crystals in certain liquids (appropriate solvents[11] as well as surfactant[12] or polymer solutions[13]). In each case, the stabilising liquid interacts with the nanosheet surface in such a way as to reduce the net exfoliation energy and stabilise the nanosheets against aggregation,[14] with considerable progress having been made to theoretically understand the stabilisation processes.[15-17] The resultant dispersions are relatively stable and can be produced at concentrations[18] up to a few $gL^{-1}$. This method produces mainly few-layer nanosheets (typically ~1-10 stacked monolayers), with monolayer contents which are low compared to the methods described above. However, post-exfoliation procedures have been described which can size-select the nanosheets and increase the monolayer content.[19, 20] Liquid phase exfoliation has an important advantage in that it is simple, scalable and cheap.[9, 21] The resultant dispersions can very easily be processed into nanostructured materials by a range of methods such as spray casting,[22] inkjet printing,[23, 24] gravure printing[25] and freeze drying.[26] These structures have been used in a wide range of applications from barrier composites[27, 28] to battery electrodes[29, 30] to photodetectors.[31, 32]

Importantly, LPE has been applied to a wide range of 2D materials including graphene,[33-35] boron nitride,[36] transition metal dichalcogenides,[10, 37, 38] transition metal oxides,[39-41] layered double hydroxides,[42] GaS,[43] phosphorene,[17, 44-47] MXenes[48] and very recently Zintl Phases.[49] The large number of layered materials which have been exfoliated to nanosheets using LPE suggests an impressive degree of versatility. This is important as the greater the versatility of an exfoliation method, the more likely it is to be useful in practical terms.

However, it is worth questioning how versatile the process really is and what are its limits. For example, the materials listed above are nominally uncharged. Conversely, many layered oxides, hydroxides and silicates are charged by virtue of mixed valence metal atoms in the basal plane.[50, 51] This means they must always be accompanied by charge balancing counter ions.[52] The presence of these counter ions might suggest that LPE cannot be used to exfoliate clays for example. Alternatively, the starting materials which have been exfoliated by LPE tend to be very pure. An interesting question is whether LPE can be used to produce nanosheets from an impure starting material or will other components dominate the exfoliated product. Recent work[53] has shown that $MoS_2$ nanosheets can be extracted from molybdenite ore by LPE. This suggests that LPE can indeed deal with impure starting materials. However, it would be worth testing the versatility of LPE further. For example, can nanosheets be extracted from other impure samples which are known to contain specific layered compounds? Can this be achieved if the layered compounds are charged? Or, more stringently, can nanosheets be isolated from unknown samples, which are merely suspected of containing layered compounds?

In this work, we explore these questions. We examine three impure starting materials, two of which – talcum powder and cat litter – were known to contain layered compounds and one – beach sand, which appeared to contain traces of clay – where the presence of layered materials was suspected. In the cat litter/sand matrix, we would expect any layered material to be layered silicates, which would be accompanied by exchangeable counterions in the interstices between negatively layers.[52] We subjected each material to a standard LPE protocol and carefully analysed the resultant material. We found that in all cases, the exfoliated material predominantly consists of nanosheets which we identify using XRD to be talc (talcum powder), bentonite and palygorskite (cat litter) and mica (beach sand). This highlights the versatility of LPE and shows that this process can extract even charged nanosheets from mixed phases.

**Results and Discussion**

Talcum powder was purchased from Boots Pharmacists (Cuticura, figure 1A) while a Fuller's earth-based cat litter was purchased from Lidl (Coshida, figure 1B). A sandy clay was collected from a beach at Parknasilla, near Sneem in Co. Kerry, Ireland (figure 1C). While Cuticura talcum powder contains talc (hydrated magnesium silicate),[54] a layered silicate, as its main ingredient, it also contains other compounds including magnesium carbonate, zinc oxide and a range of organic compounds. Coshida cat litter contains Fuller's earth,[55] a mined clay which primarily consists of layered hydrous aluminosilicates such as bentonite[56] (a subclass of

montmorillonites) and palygorskite[57] although it may also contain non-layered materials such as calcite and quartz. Prior to this project, we had no knowledge of the ingredients of the clay found at Parknasilla. However, due to its smooth, continuous texture we suspected it might contain layered silicates.

While the talcum powder and cat litter were used as received, the clay was dried and broken up into a rough powder before use (figure 1D-F). SEM analysis (figure 1 G-I) showed the talcum powder contain large quantities of platelet-like materials, presumably layered crystallites. The morphology of the cat litter sample was less clear showing particulates of a range of sizes which may or may not have been layered. SEM images of the clay showed large numbers of small platelet-like structures that appeared to sit on large continuous structures. We speculate that these represent a mixture of layered clay particles mixed with small stones or sand.

Prior knowledge of the materials, coupled with the SEM imaging described above, shows each of the three samples to contain platelets, consistent with the presence of layered crystallites. To test whether LPE can be used to exfoliate these layered crystallites, thus extracting 2D nanosheets from these starting materials, we used a standard sonication-based LPE procedure aimed at exfoliating the platelets to give nanosheets. We performed two sets of exfoliation experiments, sonicating the starting materials in pure water and in a water/surfactant solution. In line with previous results,[58] we anticipated that in both cases, the ultrasound would remove few-layer nanosheets from the layered materials present. However, it was not clear whether the resultant nanosheets would be stable in water or require the presence of a surfactant to stabilise them against aggregation. This could be ascertained by centrifugation to remove any nanosheets which were not stably dispersed as well as any non-nanosheet material.

First we washed each starting material extensively to remove molecular impurities (see methods). The resultant powder was then dried in a vacuum oven to remove residual solvent. Portions of the treated powder (1.6 g each) were sonicated in both water (80 ml) as well as a sodium cholate/water solution (80 ml, 6 mg/ml surfactant concentration) for four hours (60% amplitude, 6s on/ 2s off) to exfoliate the nanosheets. The resultant dispersions were then centrifuged for one hour at 1000 RPM and the supernatants decanted and retained (see methods for more detail).

The samples sonicated in water were very unstable. For the talc and cat litter samples, all material was removed by centrifugation, leaving a completely transparent supernatant. For

the clay, a pale dispersion remained after centrifugation. Zeta potential measurements performed immediately after centrifugation revealed a zeta potential of ~-15 mV, probably associated with the double layer of charged nanosheets and charge balancing counter ions.[52] This value is generally considered too small to give a stable dispersion. Indeed, the dispersed material sedimented completely within a few hours of centrifugation.

Conversely, the surfactant-stabilised dispersions appeared completely stable after centrifugation with the collected supernatants are shown in figure 2 A-C). This stability is in line with zeta potential measurements performed immediately after centrifugation which showed $\zeta_{talc}$=-34 mV, $\zeta_{litter}$=-23 mV, $\zeta_{clay}$=-29 mV (see SI). While these values are not particularly high, they should be high enough to impart stability on the dispersed nanosheets. We found that, in all cases, removing the surfactant by washing resulted in a fall in zeta potential to ~-15 mV and sedimentation of all dispersed material within hours (see SI).

While the talc dispersion was a milky white in colour, the cat litter and clay dispersions were much darker. We measured the optical extinction coefficient ($\varepsilon$) spectra (related to transmittance by $T = 10^{-\varepsilon C l}$, where $C$ is the nanosheet concentration and $l$ is the cell length) of the three nanosheet dispersions as shown in figure 2D ($C$ was measured by filtration and weighing, see below). These spectra are broad and featureless, as is usually found for nanostructured insulators due to the presence of light scattering.[20] To address this, we separated the extinction coefficient spectra into their inherent scattering and absorbance components using an integrating sphere.[20] The scattering coefficient ($\sigma$) spectra showed power-law behaviour in the low wavelength regime as expected (figure 2E). The absorption coefficient ($\alpha$) spectra are shown in figure 2F. In the case of talc and cat-litter, these spectra show band edges at 3.0-3.5 eV (350-400 nm), consistent with insulating behaviour but perhaps somewhat lower than the values of ~3.5 eV expected for talc[59] and >5 eV normally found for layered silicates.[60] However for clay the absorption coefficient never reached zero, even at high wavelength, implying the presence of metallic impurities.

In order to examine these dispersions by TEM a few drops of each dispersion were pipetted onto separate holey carbon grids. TEM images (figure 2 G-I) showed the presence of large quantities of 2D nanosheets in each case, with virtually no evidence of larger 3D objects (~2-3 observed per grid). This is a particularly interesting result in the case of both the cat litter and the clay as it shows that LPE is capable of extracting only the nanosheets from an inhomogeneous starting material while rejecting the larger, 3D-structured objects. Such 3D/2D

separation is probably mainly due to the fact that the nanosheets are smaller than the 3D objects typically present and is simply a case of mass separation. However, we note that 2D objects moving in a fluid feel a resistance force which increases with aspect ratio.[61] This may play a minor role in the separation process. We measured the length of the observed nanosheets (defined as the longest dimension) with histograms shown in figure 2 J-L. As is generally found for LPE, we observed broad, roughly lognormal length distributions with means of 600±40 nm, 315±29 nm and 370±22 nm for talc, cat litter and clay respectively. We also measured the nanosheet thickness distribution (expressed as number of monolayers per nanosheet) by AFM (see SI). As with nanosheet length, we observed broad lognormal distributions (figure 2 M-O) with means of 9.7±0.6, 7.4±0.3 and 8.9±0.6 for talc, cat litter and clay respectively. These thicknesses are similar to those typically observed for (non-size-selected) LPE nanosheets of standard materials such as $WS_2$ and $MoS_2$.[19, 20]

In order to estimate the mass of nanosheets exfoliated, a known volume of the dispersions were filtered onto alumina membranes using vacuum filtration. As the nanosheets were coated with sodium cholate the films were washed with 250ml of water, removing the majority of surfactant. The films were then dried in a vacuum oven and weighed. This allowed us to estimate dispersed concentrations of ~0.1 mg/ml, ~6.5 mg/ml and ~1.0 mg/ml for talc, cat litter and clay respectively (corrected for residual surfactant content as estimated by XPS, see SI). For both the cat litter and the clay these values compare very well with other 2D materials such as graphene, $MoS_2$ and $Ni(OH)_2$ which have been produced with concentrations of 2mg/ml[18], >1mg/ml[62] and 2-3mg/ml[42] respectively. The concentration of the talc is quite low but compares to values found for 2D *h*-BN in IPA of 0.06mg/ml.[63] We also collected SEM images of the surfaces of the filtered films as shown in figure 2 P-R. These images show arrays of nanosheets with almost no evidence of any non-2D structures.

It would be of interest to identify the nanosheets extracted from the three starting materials. Powder X-ray diffraction (pXRD) was performed on both starting and exfoliated materials for talcum powder, cat litter and clay with the aim of unambiguously identifying the crystalline phases present in the samples (Figure 3).

The pre-exfoliation talcum powder sample (figure 3A) gave intense reflections at 2θ ~19° and 29° with smaller peaks at a number of other angles. The pattern could be fully indexed to talc-2*M* (magnesium silicate hydroxide, ICDD # 00-019-0770, $Mg_3Si_4O_{10}(OH)_2$). There was no apparent change in this diffraction pattern in the post-exfoliation samples, suggesting

the exfoliated material to be of the same crystalline phase as the bulk (i.e. talc nanosheets) as expected.

The pXRD results for the cat litter before and after exfoliation (Figure 3B) are extremely interesting. The pXRD data of the starting material shows virtually no Bragg reflections in the pattern, suggesting it is mainly amorphous. However, when we examined the material post exfoliation, a number of reflections were observed with well-defined pair of peaks at $2\theta \sim 20°$ and 21° and an intense peak at $2\theta = 27°$. We assign the pair to the (040) and (121) planes of bentonite (ICDD # 00-003-0019), a layered clay which consists mainly of montmorillonite [$(Na,Ca)_{0.33}(Al,Mg)_2(Si_4O_{10})(OH)_2 \cdot nH_2O$] and is commonly found in cat litter. The latter intense peak can be assigned to the (231) plane of palygorskite (ICDD # 00-031-0783), again a common component of cat litter [$(Mg,Al)_2Si_4O_{10}(OH)_4(H_2O)$]. These results are important as they show that LPE can extract exfoliated nanosheets from a mixed system, while rejecting both non-exfoliated layered compounds and amorphous material.

A similarly striking purification effect was noted with the clay sample. The pXRD pattern of the pre-exfoliation, bulk material (Figure 3C) was indexed to hexagonal quartz (ICDD # 01-087-2096), which is typical for clay samples. This implies that the starting material was dominated by quartz sand with only small amounts of other crystalline materials in the sample. However, post-exfoliation, the picture is very different; we can index the pXRD pattern of the material (Figure 3C) to muscovite-2*M* (ICDD # 00-046-1311, $KAl_2(AlSi_3O_{10})(F,OH)_2$,) also known as mica, which is also a layered material.[64] This result is significant as it means that the exfoliation procedure we employ also selects between crystalline layered structures and non-layer, i.e. 3D, crystal structures.

We have confirmed our XRD assignment by XPS (see SI). We found the elemental composition of each material as measured by XPS to be consistent with the presence of the proposed structures and some residual sodium cholate. Only trivial quantities of impurity material were observed (typically Fe, Mg and Al and never more than ~3 atomic% of the total composition). This strongly supports the suggestion that LPE can effectively select the 2D materials present in mixed starting materials.

It is clear from the pXRD results that our procedure ‘selects’ and purifies crystalline nanosheets from layered bulk materials and impurity phases. This suggests that it is possible to use our exfoliation procedure on rather impure, even amorphous, ‘ores’ to produce few-layer crystalline nanosheets from the layered materials within these ‘ores’. This would be consistent

with recent work showing that $MoS_2$ nanosheets can be extracted from molybdenite ore by LPE.[53] It is clear that a wide range of naturally occurring materials and minerals could be targets for further exploration and thus exploitation.

In addition, palygorskite, bentonite and mica sheets are known to be charged due to the presence of a mixture of metal ions with different valences.[52] Such charged nanosheets are always accompanied by charge balancing counterions as mentioned above.[52] Indeed, this is why aluminasilicates can be used as sorbents for a range of metal ions by cation exchange.[65-67] The presence of the resulting double layer might suggest that standard LPE in solvents[11] may not be effective due to the impact of the double layer on the solvent-nanosheet interaction. For example, typical carbonate-intercalated layered double hydroxides (LDHs, similar to the proposed structures in this work) have not been directly exfoliated by agitation in solvents. However, this limitation is not universal as it has been shown that nitrate-intercalated LDHs (where the nitrate was introduced either by ion exchange or using specific growth techniques), can be exfoliated in solvents.[68, 69] The current work shows that, without chemical pre-treatment, surfactants can facilitate the exfoliation of layered silicates. We show that the surfactant can coat even charged nanosheets, resulting in an enhanced electrostatic stabilisation (as evidenced by the zeta potential data). However, the details of the arrangement of the surfactant molecules on the surface and their impact on the charge distribution remains unknown. We believe this is the first example of LPE being used to exfoliate charged layered crystals.

## Conclusion

In conclusion, it is clear that liquid phase exfoliation (LPE) is an extremely versatile technique to produce nanosheets from layered precursors. Here we have shown that it is possible to process naturally occurring materials such as talc, Fuller's earth cat litter and a clay/sand mix using LPE and obtain purified nanosheets while rejecting any unwanted non-2D material. What is particularly surprising is that the bentonite and palygorskite layered crystals contained in the cat litter as well as the mica in the beach sand should both consist of charged layers with charge-balancing counter ions, yet could still be exfoliated by LPE. This shows that LPE can potentially be applied to a much broader range of layered compounds than previously thought, opening the possibility of exfoliating a range of layered silicates as well as charged layered oxides and hydroxides.

## Experimental Methods

*Materials*

Talcum powder and cat litter were both purchased from Tesco and Lidl respectively. The clay was extracted form a beach in Parknasilla, Co. Kerry. Sodium cholate (SC, item no. C1254) and all solvents were purchased from Sigma Aldrich and the highest available purity.

*Preparation of Nanosheets*

As these materials have mixed composition and contain many impurities, it is necessary to introduce a treatment step to purify the powders. The materials were initially sonicated in chloroform for one hour, then centrifuged in a Hettich Mikro 220R centrifuge with a fixed-angle rotor (rotor 1016) for one hour at 4.5 kRPM (2150g) with the supernatant being decanted and discarded with the sediment being retained. This was then repeated with acetone and deionised water. The powders were then dried at $60^0$C in a vacuum oven. The pre-treated powders were sonicated in surfactant and water solution using a solid flat head sonic tip (Sonics VX-750) at 60% amplitude (6s on/ 2s off) for 4hrs. To prevent the sonic tip from overheating and potentially damaging the samples or boiling the solvent ice cooling was used. After sonication the dispersions were centrifuged (Hettich Mikro 220R) at 1000 RPM (106g) for 60 minutes. Finally, the top 75% of the dispersions were taken and kept for further analysis and characterisation.

*Characterisation and Equipment*

Optical extinction and absorbance were measured on a PerkinElmer 650 spectrometer in 0.4 cm path length quartz cuvettes. To differentiate between contributions from scattering and absorbance to the extinction spectra, dispersions were measured in an integrating sphere using a home-built sample holder to place the cuvette in the centre of the sphere (N.B. cuvettes need to be transparent to all sides and correct/reproducible positioning is important). The absorbance spectrum is obtained from the measurement inside the sphere. A second measurement on each dispersion was performed outside the sphere in the standard configuration to obtain the extinction spectrum. This allows calculation of the scattering spectrum (extinction minus absorbance).

Low-Resolution bright field transmission electron microscopy imaging was performed using a JEOL 2100, operated at 200kV. Holey carbon grids (400mesh) were purchased from Agar Scientific and prepared by diluting a dispersion to a low concentration and drop casting onto a grid placed on a filter membrane to wick away excess solvent. Statistical analysis was performed of the flake dimensions by measuring the longest axis of the flake dimensions by measuring the longest axis of the nanosheet and assigning it as ‘length’, L. Scanning electron

microscopy was performed with a Carl Zeiss Ultra SEM operating at 2kV. Images were acquired using the secondary electron detector.

AFM imaging was carried on a Veeco Nanoscope-IIIa from Digital Instruments, using e-head in tapping mode for all measurements. Nanosheets dispersions were diluted with deionized water and drop casted (15 μL) on preheated (150C) $Si/SiO_2$ wafers (0.25 $cm^2$) with an oxide layer of 300 nm. After deposition wafers were rinsed with 7 mL of deionised water, then kept in deionised water for 10 hrs and dried with condensed air prior to measurement. Typical image size taken was 12 $um^2$ for overview images and 3 $um^2$ for zoomed in images with 512 lines/image and scan rates of 0.5-0.8 Hz. Measured thickness was converted to number of layers based on conducted step height analysis of partially exfoliated nanosheets of corresponding materials. Measured step heights were 2.37 nm, 2.07 nm and 2.43 nm for clay, talc and cat litter respectively.

X-ray diffraction patterns were measured using a Bruker D8 Advance diffractometer using a copper $K_\alpha$ X-ray source (40 kV, 1.5406 Å), with a step size (2θ) of 0.04° and a dwell time of 6 s. X'Pert HighScore software (v.2.0, PANalytical BV, Netherlands) was used to match the powder patterns to known materials from the ICDD database.

Acknowledgements: We acknowledge funding from Science Foundation Ireland via the AMBER research centre (SFI/12/RC/2278) and a PI award (11/PI/1087). We are grateful for financial support from the European research Council (SEMANTICS) and the European Union Seventh Framework Programme under grant agreements n°604391 and n°696656 Graphene Flagship. JNC would like to thank Nessa, Cian and Oisin Coleman for extracting the clay from the beach at Parknasilla.

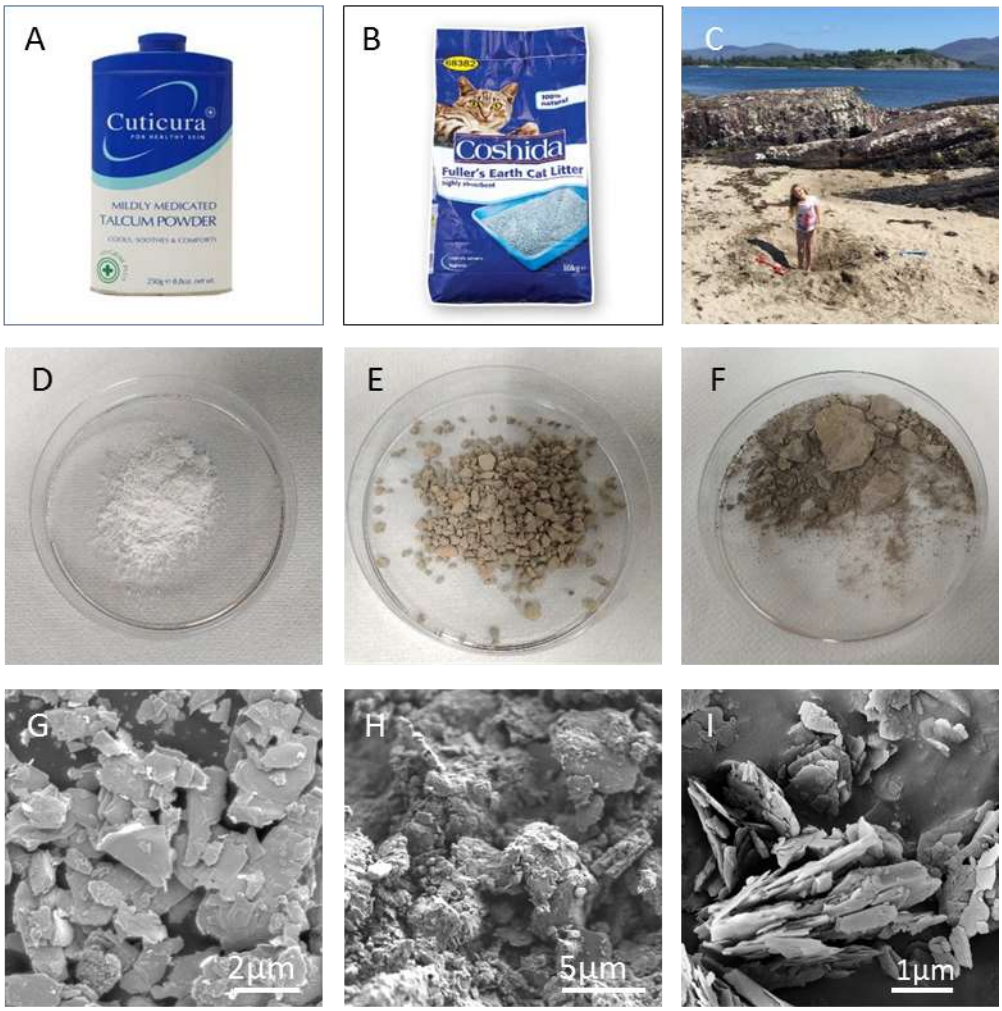


**Figure 1**: Starting material. A-C) Photographs showing the sources of the materials used in this work. A-B) Shop bought talcum powder and Fullers earth cat litter. C) The beach at Parknasilla, Co. Kerry, Ireland, where the clay was found. D-F) Photographs showing the untreated starting material: D) talcum powder, E) cat litter and F) clay. G-I) SEM images of the microstructure of the starting materials: G) talcum powder, H) cat litter and I) clay.

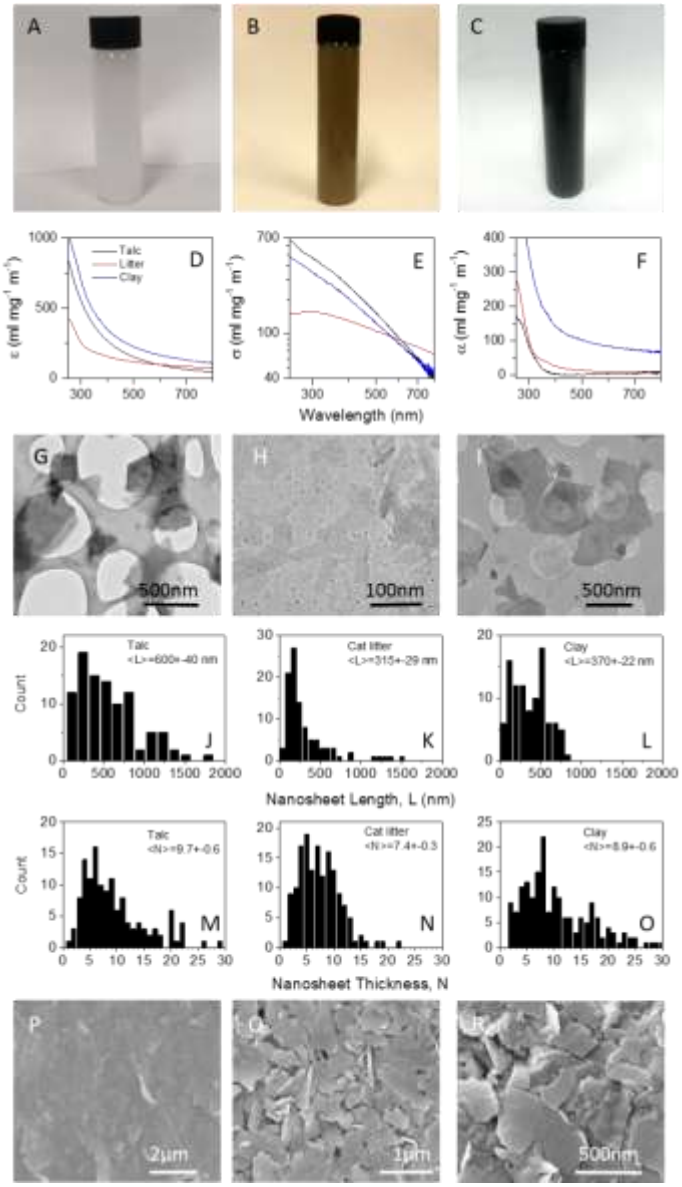


**Figure 2**: Spectroscopic and microscopic analysis of the exfoliated product. A-C) Photographs of dispersions (after centrifugation) of - A) talcum powder, B) cat litter and C) clay, all in water and stabilised by the surfactant sodium cholate ($C_{surf}$=6 mg/ml). D-F) Optical spectra for exfoliated dispersions of talc, cat-litter and clay showing D) extinction, E) scattering and F) absorption coefficient spectra. G-I) TEM images of exfoliated nanosheets extracted from each dispersion: G) talcum powder, H) cat litter and I) clay (N.B. the black dots in H are artefacts associated with the grid). J-O) Histograms showing nanosheet length (i.e. the longest dimension) distributions as measured by TEM for J) talcum powder, K) cat litter and L) clay and thickness (layer number) distributions as measured by AFM for M) talcum powder, N) cat litter and O) clay. TEM statistics were collected by counting approximately 150 nanosheets while AFM statistics employed approximately 100 counts. Uncertainties are standard errors.

P-R) SEM images of the surface of filtered films of nanosheets of P) talcum powder, Q) cat litter and R) clay.

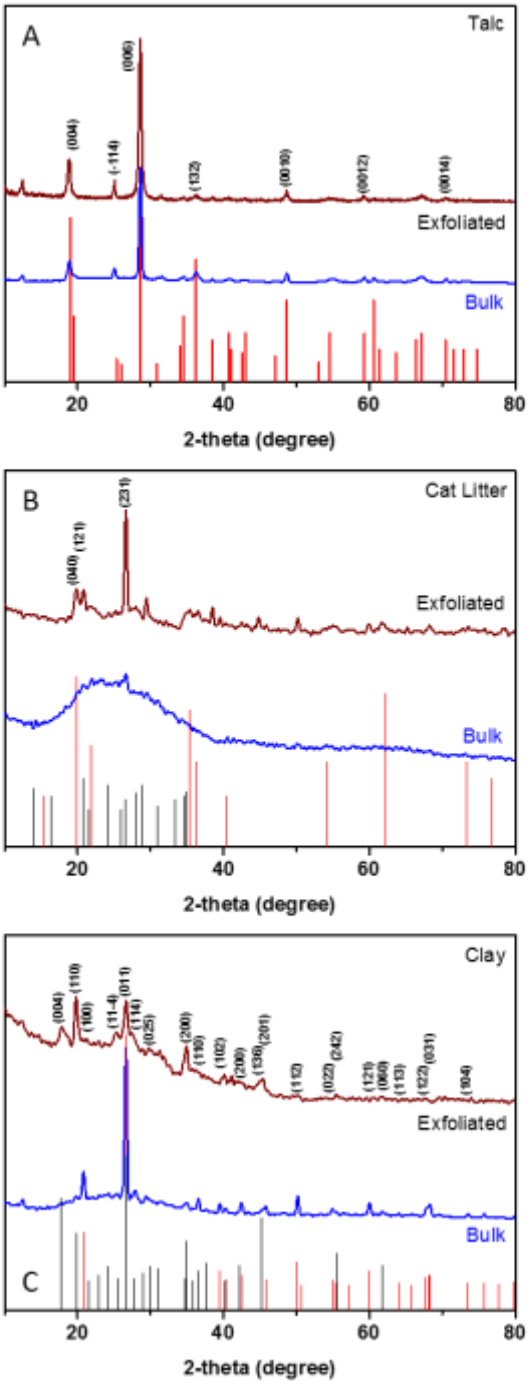


**Figure 3:** pXRD patterns of bulk and exfoliated materials. A): pXRD patterns of talcum powder and exfoliated talc nanosheets, both indexed to monoclinic talc-2*M* (red sticks, # ICDD # 00-019-0770). B) pXRD patterns of: Coshida® cat litter and (b) exfoliated nanosheets extracted from Coshida® cat litter, red and black sticks represent the standard powder patterns Bentonite (ICDD # 00-003-0019 ) orthorhombic Palygorskite (ICDD # 00-031-0783) respectively. C): pXRD patterns of clay from Parknasilla, near Sneem in Kerry, Ireland. This pattern can be indexed to hexagonal Quartz (ICDD # 01-087-2096, red sticks). Also shown is

the pXRD pattern associated with nanosheets extracted from the clay, indexed to monoclinic Muscovite-2*M* (ICDD # 00-046-1311, black sticks).


1. Chhowalla, M.; Shin, H. S.; Eda, G.; Li, L.-J.; Loh, K. P.; Zhang, H., The Chemistry of Two-Dimensional Layered Transition Metal Dichalcogenide Nanosheets. *Nature Chemistry* **2013,** 5, 263-275.
2. Nicolosi, V.; Chhowalla, M.; Kanatzidis, M. G.; Strano, M. S.; Coleman, J. N., Liquid Exfoliation of Layered Materials. *Science (Washington, DC, United States)* **2013,** 340, 1420-+.
3. Wang, Q. H.; Kalantar-Zadeh, K.; Kis, A.; Coleman, J. N.; Strano, M. S., Electronics and Optoelectronics of Two-Dimensional Transition Metal Dichalcogenides. *Nature Nanotechnology* **2012,** 7, 699-712.
4. Young, R. J.; Kinloch, I. A.; Gong, L.; Novoselov, K. S., The Mechanics of Graphene Nanocomposites: A Review. *Composites Science and Technology* **2012,** 72, 1459-1476.
5. Torrisi, F.; Coleman, J. N., Electrifying Inks with 2d Materials. *Nature Nanotechnology* **2014,** 9, 738-739.
6. Acerce, M.; Voiry, D.; Chhowalla, M., Metallic 1t Phase Mos2 Nanosheets as Supercapacitor Electrode Materials. *Nature Nanotechnology* **2015,** 10, 313-318.
7. Bonaccorso, F.; Bartolotta, A.; Coleman, J. N.; Backes, C., 2d-Crystal-Based Functional Inks. *Adv Mater* **2016,** 28, 6136-6166.
8. Niu, L. Y.; Coleman, J. N.; Zhang, H.; Shin, H.; Chhowalla, M.; Zheng, Z. J., Production of Two-Dimensional Nanomaterials Via Liquid-Based Direct Exfoliation. *Small* **2016,** 12, 272-293.
9. Paton, K. R.; Varrla, E.; Backes, C.; Smith, R. J.; Khan, U.; O'Neill, A.; Boland, C.; Lotya, M.; Istrate, O. M.; King, P.; Higgins, T.; Barwich, S.; May, P.; Puczkarski, P.; Ahmed, I.; Moebius, M.; Pettersson, H.; Long, E.; Coelho, J.; O'Brien, S. E., *et al.*, Scalable Production of Large Quantities of Defect-Free Few-Layer Graphene by Shear Exfoliation in Liquids. *Nat Mater* **2014,** 13, 624-630.
10. Coleman, J. N.; Lotya, M.; O'Neill, A.; Bergin, S. D.; King, P. J.; Khan, U.; Young, K.; Gaucher, A.; De, S.; Smith, R. J.; Shvets, I. V.; Arora, S. K.; Stanton, G.; Kim, H.-Y.; Lee, K.; Kim, G. T.; Duesberg, G. S.; Hallam, T.; Boland, J. J.; Wang, J. J., *et al.*, Two-Dimensional Nanosheets Produced by Liquid Exfoliation of Layered Materials. *Science (Washington, DC, United States)* **2011,** 331, 568-571.
11. Cunningham, G.; Lotya, M.; Cucinotta, C. S.; Sanvito, S.; Bergin, S. D.; Menzel, R.; Shaffer, M. S. P.; Coleman, J. N., Solvent Exfoliation of Transition Metal Dichalcogenides: Dispersibility of Exfoliated Nanosheets Varies Only Weakly between Compounds. *Acs Nano* **2012,** 6, 3468-3480.
12. Smith, R. J.; King, P. J.; Lotya, M.; Wirtz, C.; Khan, U.; De, S.; O'Neill, A.; Duesberg, G. S.; Grunlan, J. C.; Moriarty, G.; Chen, J.; Wang, J. Z.; Minett, A. I.; Nicolosi, V.; Coleman, J. N., Large-Scale Exfoliation of Inorganic Layered Compounds in Aqueous Surfactant Solutions. *Adv Mater* **2011,** 23, 3944-+.
13. May, P.; Khan, U.; Hughes, J. M.; Coleman, J. N., Role of Solubility Parameters in Understanding the Steric Stabilization of Exfoliated Two-Dimensional Nanosheets by Adsorbed Polymers. *Journal of Physical Chemistry C* **2012,** 116, 11393-11400.
14. Coleman, J. N., Liquid Exfoliation of Defect-Free Graphene. *Accounts of Chemical Research* **2013,** 46, 14-22.
15. Shih, C. J.; Lin, S. C.; Strano, M. S.; Blankschtein, D., Understanding the Stabilization of Liquid-Phase-Exfoliated Graphene in Polar Solvents: Molecular Dynamics Simulations and Kinetic Theory of Colloid Aggregation. *Journal of the American Chemical Society* **2010,** 132, 14638-14648.
16. Shih, C. J.; Lin, S. C.; Strano, M. S.; Blankschtein, D., Understanding the Stabilization of Single-Walled Carbon Nanotubes and Graphene in Ionic Surfactant Aqueous Solutions: Large-Scale Coarse-Grained Molecular Dynamics Simulation-Assisted Dlvo Theory. *Journal of Physical Chemistry C* **2015,** 119, 1047-1060.

17. Sreshtt, V.; Padua, A. A. H.; Blankschtein, D., Liquid-Phase Exfoliation of Phosphorene: Design Rules from Molecular Dynamics Simulations. *Acs Nano* **2015,** 9, 8255-8268.
18. Khan, U.; Porwal, H.; O'Neill, A.; Nawaz, K.; May, P.; Coleman, J. N., Solvent-Exfoliated Graphene at Extremely High Concentration. *Langmuir* **2011,** 27, 9077-9082.
19. Backes, C.; Szydlowska, B. M.; Harvey, A.; Yuan, S.; Vega-Mayoral, V.; Davies, B. R.; Zhao, P. L.; Hanlon, D.; Santos, E. J.; Katsnelson, M. I.; Blau, W. J.; Gadermaier, C.; Coleman, J. N., Production of Highly Monolayer Enriched Dispersions of Liquid-Exfoliated Nanosheets by Liquid Cascade Centrifugation. *ACS Nano* **2016,** 10, 1589-601.
20. Backes, C.; Smith, R. J.; McEvoy, N.; Berner, N. C.; McCloskey, D.; Nerl, H. C.; O'Neill, A.; King, P. J.; Higgins, T.; Hanlon, D.; Scheuschner, N.; Maultzsch, J.; Houben, L.; Duesberg, G. S.; Donegan, J. F.; Nicolosi, V.; Coleman, J. N., Edge and Confinement Effects Allow in Situ Measurement of Size and Thickness of Liquid-Exfoliated Nanosheets. *Nat Commun* **2014,** 5.
21. Yi, M.; Shen, Z., Kitchen Blender for Producing High-Quality Few-Layer Graphene. *Carbon* **2014,** 78, 622-626.
22. Mendoza-Sanchez, B.; Coelho, J.; Pokle, A.; Nicolosi, V., A 2d Graphene-Manganese Oxide Nanosheet Hybrid Synthesized by a Single Step Liquid-Phase Co-Exfoliation Method for Supercapacitor Applications. *Electrochim. Acta* **2015,** 174, 696-705.
23. Finn, D. J.; Lotya, M.; Cunningham, G.; Smith, R. J.; McCloskey, D.; Donegan, J. F.; Coleman, J. N., Inkjet Deposition of Liquid-Exfoliated Graphene and Mos2 Nanosheets for Printed Device Applications. *Journal of Materials Chemistry C* **2014,** 2, 925-932.
24. Torrisi, F.; Hasan, T.; Wu, W. P.; Sun, Z. P.; Lombardo, A.; Kulmala, T. S.; Hsieh, G. W.; Jung, S. J.; Bonaccorso, F.; Paul, P. J.; Chu, D. P.; Ferrari, A. C., Inkjet-Printed Graphene Electronics. *Acs Nano* **2012,** 6, 2992-3006.
25. Secor, E. B.; Lim, S.; Zhang, H.; Frisbie, C. D.; Francis, L. F.; Hersam, M. C., Gravure Printing of Graphene for Large-Area Flexible Electronics. *Adv Mater* **2014,** 26, 4533-+.
26. Zhang, X. T.; Sui, Z. Y.; Xu, B.; Yue, S. F.; Luo, Y. J.; Zhan, W. C.; Liu, B., Mechanically Strong and Highly Conductive Graphene Aerogel and Its Use as Electrodes for Electrochemical Power Sources. *J Mater Chem* **2011,** 21, 6494-6497.
27. Biscarat, J.; Bechelany, M.; Pochat-Bohatier, C.; Miele, P., Graphene-Like Bn/Gelatin Nanobiocomposites for Gas Barrier Applications. *Nanoscale* **2015,** 7, 613-618.
28. Xie, S.; Istrate, O. M.; May, P.; Barwich, S.; Bell, A. P.; Khana, U.; Coleman, J. N., Boron Nitride Nanosheets as Barrier Enhancing Fillers in Melt Processed Composites. *Nanoscale* **2015,** 7, 4443-4450.
29. Sun, J.; Lee, H.-W.; Pasta, M.; Yuan, H.; Zheng, G.; Sun, Y.; Li, Y.; Cui, Y., A Phosphorene–Graphene Hybrid Material as a High-Capacity Anode for Sodium-Ion Batteries. *Nat Nano* **2015,** 10, 980-985.
30. Sun, H. Y.; Castillo, A. E. D.; Monaco, S.; Capasso, A.; Ansaldo, A.; Prato, M.; Dinh, D. A.; Pellegrini, V.; Scrosati, B.; Manna, L.; Bonaccorso, F., Binder-Free Graphene as an Advanced Anode for Lithium Batteries. *Journal of Materials Chemistry A* **2016,** 4, 6886-6895.
31. Cunningham, G.; Hanlon, D.; McEvoy, N.; Duesberg, G. S.; Coleman, J. N., Large Variations in Both Dark- and Photoconductivity in Nanosheet Networks as Nanomaterial Is Varied from Mos2 to Wte2. *Nanoscale* **2014,** 7, 198-208.
32. Withers, F.; Yang, H.; Britnell, L.; Rooney, A. P.; Lewis, E.; Felten, A.; Woods, C. R.; Sanchez Romaguera, V.; Georgiou, T.; Eckmann, A.; Kim, Y. J.; Yeates, S. G.; Haigh, S. J.; Geim, A. K.; Novoselov, K. S.; Casiraghi, C., Heterostructures Produced from Nanosheet-Based Inks. *Nano Letters* **2014,** 14, 3987-3992.
33. Hernandez, Y.; Nicolosi, V.; Lotya, M.; Blighe, F. M.; Sun, Z.; De, S.; McGovern, I. T.; Holland, B.; Byrne, M.; Gun'ko, Y. K.; Boland, J. J.; Niraj, P.; Duesberg, G.; Krishnamurthy, S.; Goodhue, R.; Hutchison, J.; Scardaci, V.; Ferrari, A. C.; Coleman, J. N., High-Yield Production of Graphene by Liquid-Phase Exfoliation of Graphite. *Nature Nanotechnology* **2008,** 3, 563-568.
34. Liu, L. H.; Zorn, G.; Castner, D. G.; Solanki, R.; Lerner, M. M.; Yan, M. D., A Simple and Scalable Route to Wafer-Size Patterned Graphene. *J Mater Chem* **2010,** 20, 5041-5046.
35. Du, W. C.; Lu, J.; Sun, P. P.; Zhu, Y. Y.; Jiang, X. Q., Organic Salt-Assisted Liquid-Phase Exfoliation of Graphite to Produce High-Quality Graphene. *Chem Phys Lett* **2013,** 568, 198-201.

36. Zhi, C. Y.; Bando, Y.; Tang, C. C.; Kuwahara, H.; Golberg, D., Large-Scale Fabrication of Boron Nitride Nanosheets and Their Utilization in Polymeric Composites with Improved Thermal and Mechanical Properties. *Adv Mater* **2009,** 21, 2889-+.
37. Bang, G. S.; Nam, K. W.; Kim, J. Y.; Shin, J.; Choi, J. W.; Choi, S. Y., Effective Liquid-Phase Exfoliation and Sodium Ion Battery Application of Mos2 Nanosheets. *Acs Appl Mater Inter* **2014,** 6, 7084-7089.
38. Bernal, M. M.; Alvarez, L.; Giovanelli, E.; Arnaiz, A.; Ruiz-Gonzalez, L.; Casado, S.; Granados, D.; Pizarro, A. M.; Castellanos-Gomez, A.; Perez, E. M., Luminescent Transition Metal Dichalcogenide Nanosheets through One-Step Liquid Phase Exfoliation. *2D Mater.* **2016,** 3, 11.
39. Hanlon, D.; Backes, C.; Higgins, T. M.; Hughes, M.; O'Neill, A.; King, P.; McEvoy, N.; Duesberg, G. S.; Sanchez, B. M.; Pettersson, H.; Nicolosi, V.; Coleman, J. N., Production of Molybdenum Trioxide Nanosheets by Liquid Exfoliation and Their Application in High-Performance Supercapacitors. *Chem Mater* **2014,** 26, 1751-1763.
40. Alsaif, M. M. Y. A.; Balendhran, S.; Field, M. R.; Latham, K.; Wlodarski, W.; Ou, J. Z.; Kalantar-Zadeh, K., Two Dimensional Alpha-Moo3 Nanoflakes Obtained Using Solvent-Assisted Grinding and Sonication Method: Application for H-2 Gas Sensing. *Sensor Actuat B-Chem* **2014,** 192, 196-204.
41. Zhang, H. J.; Gao, L. J.; Gong, Y. J., Exfoliated Moo3 Nanosheets for High-Capacity Lithium Storage. *Electrochem. Commun.* **2015,** 52, 67-70.
42. Harvey, A.; He, X. Y.; Godwin, I. J.; Backes, C.; McAteer, D.; Berner, N. C.; McEvoy, N.; Ferguson, A.; Shmeliov, A.; Lyons, M. E. G.; Nicolosi, V.; Duesberg, G. S.; Donegan, J. F.; Coleman, J. N., Production of Ni(Oh)(2) Nanosheets by Liquid Phase Exfoliation: From Optical Properties to Electrochemical Applications. *Journal of Materials Chemistry A* **2016,** 4, 11046-11059.
43. Harvey, A.; Backes, C.; Gholamvand, Z.; Hanlon, D.; McAteer, D.; Nerl, H. C.; McGuire, E.; Seral-Ascaso, A.; Ramasse, Q. M.; McEvoy, N.; Winters, S.; Berner, N. C.; McCloskey, D.; Donegan, J. F.; Duesberg, G. S.; Nicolosi, V.; Coleman, J. N., Preparation of Gallium Sulfide Nanosheets by Liquid Exfoliation and Their Application as Hydrogen Evolution Catalysts. *Chem Mater* **2015,** 27, 3483-3493.
44. Kang, J.; Wood, J. D.; Wells, S. A.; Lee, J.-H.; Liu, X.; Chen, K.-S.; Hersam, M. C., Solvent Exfoliation of Electronic-Grade, Two-Dimensional Black Phosphorus. *Acs Nano* **2015,** 9, 3596-3604.
45. Yasaei, P.; Kumar, B.; Foroozan, T.; Wang, C.; Asadi, M.; Tuschel, D.; Indacochea, J. E.; Klie, R. F.; Salehi-Khojin, A., High-Quality Black Phosphorus Atomic Layers by Liquid-Phase Exfoliation. *Adv Mater* **2015,** 27, 1887-+.
46. Hanlon, D.; Backes, C.; Doherty, E.; Cucinotta, C. S.; Berner, N. C.; Boland, C.; Lee, K.; Harvey, A.; Lynch, P.; Gholamvand, Z.; Zhang, S. F.; Wang, K. P.; Moynihan, G.; Pokle, A.; Ramasse, Q. M.; McEvoy, N.; Blau, W. J.; Wang, J.; Abellan, G.; Hauke, F., *et al.*, Liquid Exfoliation of Solvent-Stabilized Few-Layer Black Phosphorus for Applications Beyond Electronics. *Nat Commun* **2015,** 6.
47. Brent, J. R.; Savjani, N.; Lewis, E. A.; Haigh, S. J.; Lewis, D. J.; O'Brien, P., Production of Few-Layer Phosphorene by Liquid Exfoliation of Black Phosphorus. *Chemical Communications* **2014,** 50, 13338-13341.
48. Naguib, M.; Mashtalir, O.; Carle, J.; Presser, V.; Lu, J.; Hultman, L.; Gogotsi, Y.; Barsoum, M. W., Two-Dimensional Transition Metal Carbides. *Acs Nano* **2012,** 6, 1322-1331.
49. Arguilla, M. Q.; Katoch, J.; Krymowski, K.; Cultrara, N. D.; Xu, J.; Xi, X.; Hanks, A.; Jiang, S.; Ross, R. D.; Koch, R. J.; Ulstrup, S.; Bostwick, A.; Jozwiak, C.; McComb, D. W.; Rotenberg, E.; Shan, J.; Windl, W.; Kawakami, R. K.; Goldberger, J. E., Nasn2as2: An Exfoliatable Layered Van Der Waals Zintl Phase. *ACS Nano* **2016**.
50. Ma, R. Z.; Sasaki, T., Nanosheets of Oxides and Hydroxides: Ultimate 2d Charge-Bearing Functional Crystallites. *Adv Mater* **2010,** 22, 5082-5104.
51. Osada, M.; Sasaki, T., Two-Dimensional Dielectric Nanosheets: Novel Nanoelectronics from Nanocrystal Building Blocks. *Adv Mater* **2012,** 24, 210-228.
52. Luckham, P. F.; Rossi, S., The Colloidal and Rheological Properties of Bentonite Suspensions. *Advances in Colloid and Interface Science* **1999,** 82, 43-92.
53. Savjani, N.; Lewis, E. A.; Pattrick, R. A. D.; Haigh, S. J.; O'Brien, P., Mos2 Nanosheet Production by the Direct Exfoliation of Molybdenite Minerals from Several Type-Localities. *Rsc Advances* **2014,** 4, 35609-35613.

54. Rayner, J. H.; Brown, G., Crystal-Structure of Talc. *Clays and Clay Minerals* **1973,** 21, 103-114.
55. Ruffell, A. H.; Hesselbo, S. P.; Wach, G. D.; Simpson, M. I.; Wray, D. S., Fuller's Earth (Bentonite) in the Lower Cretaceous (Upper Aptian) of Shanklin (Isle of Wight, Southern England). *Proc. Geol. Assoc.* **2002,** 113, 281-290.
56. Eisenhour, D. D.; Brown, R. K., Bentonite and Its Impact on Modern Life. *Elements* **2009,** 5, 83-88.
57. Murray, H. H., Traditional and New Applications for Kaolin, Smectite, and Palygorskite: A General Overview. *Applied Clay Science* **2000,** 17, 207-221.
58. Barwich, S.; Khan, U.; Coleman, J. N., A Technique to Pretreat Graphite Which Allows the Rapid Dispersion of Defect-Free Graphene in Solvents at High Concentration. *Journal of Physical Chemistry C* **2013,** 117, 19212-19218.
59. Sayre, R. M.; Kollias, N.; Roberts, R. L.; Baqer, A.; Sadiq, I., Physical Sunscreens. *Journal of the Society of Cosmetic Chemists* **1990,** 41, 103-109.
60. He, M. C.; Fang, Z. J.; Zhang, P., Atomic and Electronic Structures of Montmorillonite in Soft Rock. *Chinese Physics B* **2009,** 18, 2933-2937.
61. Van Holde, K. E., *Physical Biochemistry*. Prentice-Hall: 1971.
62. O'Neill, A.; Khan, U.; Coleman, J. N., Preparation of High Concentration Dispersions of Exfoliated Mos2 with Increased Flake Size. *Chem Mater* **2012,** 24, 2414-2421.
63. Coleman, J. N.; Lotya, M.; O'Neill, A.; Bergin, S. D.; King, P. J.; Khan, U.; Young, K.; Gaucher, A.; De, S.; Smith, R. J.; Shvets, I. V.; Arora, S. K.; Stanton, G.; Kim, H. Y.; Lee, K.; Kim, G. T.; Duesberg, G. S.; Hallam, T.; Boland, J. J.; Wang, J. J., *et al.*, Two-Dimensional Nanosheets Produced by Liquid Exfoliation of Layered Materials. *Science* **2011,** 331, 568-571.
64. Yoder, H. S.; Eugster, H. P., Synthetic and Natural Muscovites. *Geochimica Et Cosmochimica Acta* **1955,** 8, 225-&.
65. Abollino, O.; Aceto, M.; Malandrino, M.; Sarzanini, C.; Mentasti, E., Adsorption of Heavy Metals on Na-Montmorillonite. Effect of Ph and Organic Substances. *Water Research* **2003,** 37, 1619-1627.
66. Alvarez-Ayuso, E.; Garcia-Sanchez, A., Removal of Heavy Metals from Waste Waters by Natural and Na-Exchanged Bentonites. *Clays and Clay Minerals* **2003,** 51, 475-480.
67. Bailey, S. E.; Olin, T. J.; Bricka, R. M.; Adrian, D. D., A Review of Potentially Low-Cost Sorbents for Heavy Metals. *Water Research* **1999,** 33, 2469-2479.
68. Li, L.; Ma, R. Z.; Ebina, Y.; Iyi, N.; Sasaki, T., Positively Charged Nanosheets Derived Via Total Delamination of Layered Double Hydroxides. *Chem Mater* **2005,** 17, 4386-4391.
69. Zhao, Y.; Yang, W. D.; Xue, Y. H.; Wang, X. G.; Lin, T., Partial Exfoliation of Layered Double Hydroxides in Dmso: A Route to Transparent Polymer Nanocomposites. *J Mater Chem* **2011,** 21, 4869-4874.